

UC Berkeley

UC Berkeley Previously Published Works

Title

Improving photosynthesis and crop productivity by accelerating recovery from photoprotection

Permalink

<https://escholarship.org/uc/item/1xt5762k>

Journal

Science, 354(6314)

ISSN

0036-8075

Authors

Kromdijk, Johannes
Głowacka, Katarzyna
Leonelli, Lauriebeth
[et al.](#)

Publication Date

2016-11-18

DOI

10.1126/science.aai8878

Peer reviewed

REFERENCES AND NOTES

- S. D. Roughley, A. M. Jordan, *J. Med. Chem.* **54**, 3451–3479 (2011).
- R. N. Salvatore, C. H. Yoon, K. W. Jung, *Tetrahedron* **57**, 7785–7811 (2001).
- E. W. Baxter, A. B. Reitz, *Org. React.* **59**, 1–714 (2004).
- J. Bariwal, E. Van der Eycken, *Chem. Soc. Rev.* **42**, 9283–9303 (2013).
- D. S. Surry, S. L. Buchwald, *Angew. Chem. Int. Ed. Engl.* **47**, 6338–6361 (2008).
- J. F. Hartwig, *Acc. Chem. Res.* **41**, 1534–1544 (2008).
- Y. Yang, S.-L. Shi, D. Niu, P. Liu, S. L. Buchwald, *Science* **349**, 62–66 (2015).
- J. Gui *et al.*, *Science* **348**, 886–891 (2015).
- C. K. Savile *et al.*, *Science* **329**, 305–309 (2010).
- F. G. Mutti, T. Knaus, N. S. Scrutton, M. Breuer, N. J. Turner, *Science* **349**, 1525–1529 (2015).
- J. Yamaguchi, A. D. Yamaguchi, K. Itami, *Angew. Chem. Int. Ed. Engl.* **51**, 8960–9009 (2012).
- T. W. Lyons, M. S. Sanford, *Chem. Rev.* **110**, 1147–1169 (2010).
- I. A. I. Mkhaliid, J. H. Barnard, T. B. Marder, J. M. Murphy, J. F. Hartwig, *Chem. Rev.* **110**, 890–931 (2010).
- J. Wencel-Delord, T. Dröge, F. Liu, F. Glorius, *Chem. Soc. Rev.* **40**, 4740–4761 (2011).
- R. Jazzar, J. Hitce, A. Renaudat, J. Sofack-Kreutzer, O. Baudoin, *Chemistry* **16**, 2654–2672 (2010).
- H. A. Chiong, Q. N. Pham, O. Daugulis, *J. Am. Chem. Soc.* **129**, 9879–9884 (2007).
- K. M. Engle, T. S. Mei, M. Wasa, J.-Q. Yu, *Acc. Chem. Res.* **45**, 788–802 (2012).
- K. J. Stowers, K. C. Fortner, M. S. Sanford, *J. Am. Chem. Soc.* **133**, 6541–6544 (2011).
- E. M. Simmons, J. F. Hartwig, *Nature* **483**, 70–73 (2012).
- A. D. Ryabov, *Chem. Rev.* **90**, 403–424 (1990).
- K. S. L. Chan *et al.*, *Nat. Chem.* **6**, 146–150 (2014).
- V. G. Zaitsev, D. Shabashov, O. Daugulis, *J. Am. Chem. Soc.* **127**, 13154–13155 (2005).
- G. He, G. Chen, *Angew. Chem. Int. Ed. Engl.* **50**, 5192–5196 (2011).
- C. Wang *et al.*, *Chem. Sci.* **6**, 4610–4614 (2015).
- J. J. Topczewski, P. J. Cabrera, N. I. Saper, M. S. Sanford, *Nature* **531**, 220–224 (2016).
- A. McNally, B. Haffemayer, B. S. L. Collins, M. J. Gaunt, *Nature* **510**, 129–133 (2014).
- J. Calleja *et al.*, *Nat. Chem.* **7**, 1009–1016 (2015).
- X.-F. Wu, H. Neumann, M. Beller, *ChemSusChem* **6**, 229–241 (2013).
- C. Jia, T. Kitamura, Y. Fujiwara, *Acc. Chem. Res.* **34**, 633–639 (2001).
- We considered a number of alternative pathways as part of our assessment of possible catalytic cycles. See the supplementary materials for details of these calculations.
- T. A. Stromnova, M. N. Vargaftik, I. I. Moiseev, *J. Organomet. Chem.* **252**, 113–120 (1983).
- K. Orito *et al.*, *J. Am. Chem. Soc.* **126**, 14342–14343 (2004).
- E. J. Yoo, M. Wasa, J.-Q. Yu, *J. Am. Chem. Soc.* **132**, 17378–17380 (2010).
- K. L. Hull, M. S. Sanford, *J. Am. Chem. Soc.* **131**, 9651–9653 (2009).
- J. He *et al.*, *Science* **343**, 1216–1220 (2014).
- C. Tsukano, M. Okuno, Y. Takemoto, *Angew. Chem. Int. Ed. Engl.* **51**, 2763–2766 (2012).
- B. V. Popp, S. S. Stahl, *Chemistry* **15**, 2915–2922 (2009).
- Y.-J. Liu *et al.*, *Nature* **515**, 389–393 (2015).
- W. Li *et al.*, *Angew. Chem. Int. Ed. Engl.* **54**, 1893–1896 (2015).
- N. A. McGrath, M. Brichacek, J. T. Njardarson, *J. Chem. Educ.* **87**, 1348–1349 (2010).
- J. Wencel-Delord, F. Glorius, *Nat. Chem.* **5**, 369–375 (2013).
- D. Nedelcu, J. Liu, Y. Xu, C. Jao, A. Salic, *Nat. Chem. Biol.* **9**, 557–564 (2013).
- B. K. Banik, Ed., *β -Lactams: Unique Structures of Distinction for Novel Molecules* (Springer, 2013).

ACKNOWLEDGMENTS

We gratefully acknowledge funding from the European Research Council and the UK Engineering and Physical Sciences Research

Council (EPSRC) (to D.W., K.F.H., A.P.S., and M.J.G.), the Herchel Smith Trust (to B.G.N.C.), the Marie Curie Foundation (to J.C.), and the Royal Society (Wolfson Merit Award to M.J.G.). Mass spectrometry data were acquired at the EPSRC UK National Mass Spectrometry Facility at Swansea University. Computational work was performed with the Darwin Supercomputer of the University of Cambridge High Performance Computing Service (<http://www.hpc.cam.ac.uk/>), provided by Dell, using Strategic Research Infrastructure Funding from the Higher Education Funding Council for England. The supplementary materials contain ^1H and ^{13}C NMR spectra and computational details. Crystallographic data are available free of charge from the Cambridge

Crystallographic Data Centre under reference numbers CCDC-1508626 to CCDC-1508631.

SUPPLEMENTARY MATERIALS

www.sciencemag.org/content/354/6314/851/suppl/DC1
Materials and Methods
Figs. S1 to S3
NMR Spectra
References (44–55)

26 April 2016; accepted 13 October 2016
10.1126/science.aaf9621

PLANT SCIENCE

Improving photosynthesis and crop productivity by accelerating recovery from photoprotection

Johannes Kromdijk,^{1*} Katarzyna Głowacka,^{1,2*} Lauriebeth Leonelli,³ Stéphane T. Gabilly,³ Masakazu Iwai,^{3,4} Krishna K. Niyogi,^{3,4,†} Stephen P. Long^{1,5,†}

Crop leaves in full sunlight dissipate damaging excess absorbed light energy as heat. When sunlit leaves are shaded by clouds or other leaves, this protective dissipation continues for many minutes and reduces photosynthesis. Calculations have shown that this could cost field crops up to 20% of their potential yield. Here, we describe the bioengineering of an accelerated response to natural shading events in *Nicotiana* (tobacco), resulting in increased leaf carbon dioxide uptake and plant dry matter productivity by about 15% in fluctuating light. Because the photoprotective mechanism that has been altered is common to all flowering plants and crops, the findings provide proof of concept for a route to obtaining a sustainable increase in productivity for food crops and a much-needed yield jump.

According to detailed forecasts of future global food demand, current rates of increase in crop yields per hectare of land are inadequate. Prior model predictions have suggested that the efficiency of the photosynthetic process and thereby crop yield could be improved (1). Here, we show improvement of photosynthetic efficiency and crop productivity through genetic manipulation of photoprotection.

Light in plant canopies is very dynamic, and leaves routinely experience sharp fluctuations in levels of absorbed irradiance. When light intensity is too high or increases too fast for photochemistry to use the absorbed energy, several photoprotective mechanisms are induced to protect the photosynthetic antenna complexes from overexcitation (2). Excess excitation energy in

the photosystem II (PSII) antenna complex can be harmlessly dissipated as heat, which is observable as a process named nonphotochemical quenching of chlorophyll fluorescence (NPQ) (3). Changes in NPQ can be fast but are not instantaneous and therefore lag behind fluctuations in absorbed irradiance. In particular, the rate of NPQ relaxation is slower than the rate of induction, and this asymmetry is exacerbated by prolonged or repeated exposure to excessive light conditions (4). This slow rate of recovery of PSII antennae from the quenched to the unquenched state implies that the photosynthetic quantum yield of CO₂ fixation is transiently depressed by NPQ upon a transition from high to low light intensity (Fig. 1). When this hypothesis was tested in model simulations and integrated for a crop canopy over a diurnal course, corresponding losses of CO₂ fixation were estimated to range between 7.5 and 30% (5–7). On the basis of these computations, increasing the relaxation rate of NPQ appeared to be a very promising strategy for improving crop photosynthetic efficiency and in turn yield (8).

Although the exact NPQ quenching site and nature of the quenching mechanisms involved are still debated (9), it is clear that for NPQ to occur, PSII-associated antennae need to undergo a conformational change to the quenched state,

¹Carl R. Woese Institute for Genomic Biology, University of Illinois, 1206 West Gregory Drive, Urbana, IL 61801, USA.

²Institute of Plant Genetics, Polish Academy of Sciences, Ulica Strzeszyńska 34, 60-479 Poznań, Poland. ³Howard Hughes Medical Institute, Department of Plant and Microbial Biology, 111 Koshland Hall, University of California Berkeley, Berkeley, CA 94720-3102, USA. ⁴Molecular Biophysics and Integrated Bioimaging Division, Lawrence Berkeley National Laboratory, Berkeley, CA 94720, USA. ⁵Lancaster Environment Centre, University of Lancaster, Lancaster, LA1 1YX, UK.

*These authors contributed equally to this work. †Corresponding author. Email: niyogi@berkeley.edu (K.K.N.); slong@illinois.edu (S.P.L.)

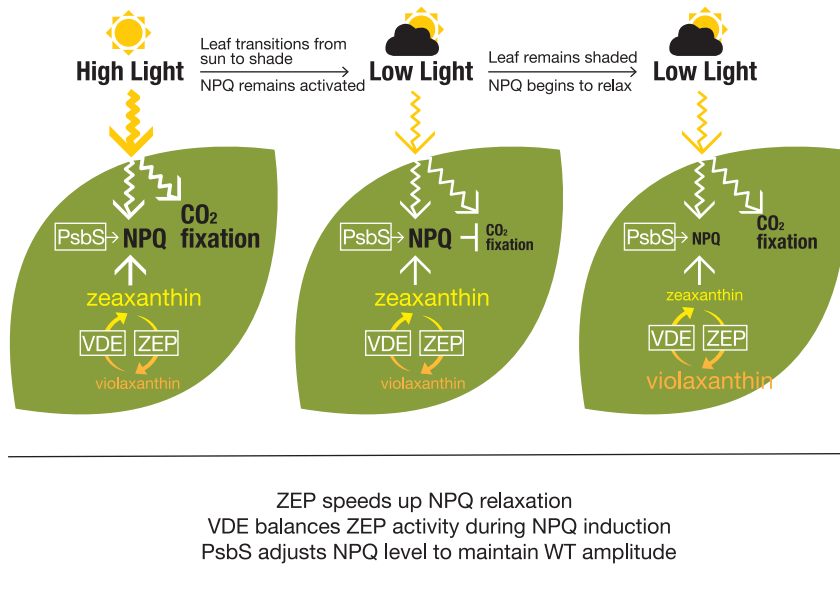


Fig. 1. Interaction between photoprotection and CO₂ fixation during sun-shade transitions.

When leaves are exposed to high light, the rate of CO₂ fixation is high, and excessive excitation energy is harmlessly dissipated through NPQ. The level of NPQ is positively correlated with the abundance of PsbS and further stimulated by the de-epoxidation of violaxanthin to zeaxanthin, catalyzed by VDE. Upon transition to low light, CO₂ fixation becomes limited by the reduced form of nicotinamide adenine dinucleotide phosphate and adenosine triphosphate derived from photosynthetic electron transport, which in turn is limited by high levels of NPQ. The rate of CO₂ fixation therefore remains depressed until relaxation of NPQ is complete. This can take minutes to hours and is correlated with the rate of zeaxanthin epoxidation, catalyzed by ZEP. The text underneath the figure describes the strategy used to accelerate NPQ relaxation compared with WT tobacco.

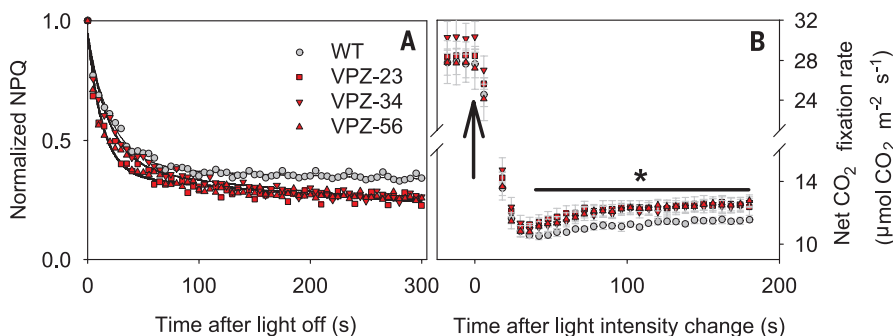


Fig. 3. Transient adjustment of NPQ and net CO₂ assimilation. (A) Dark relaxation of NPQ after exposure to alternating high and low light in young seedlings of wild-type *N. tabacum* (WT) and three lines expressing *AtVDE*, *AtPsbS*, and *AtZEP* (VPZ). Lines depict best fits of a double exponential model for WT ($\tau_1 = 21.4 \pm 1.2$ s and $\tau_2 = 2641.1 \pm 821.2$ s), VPZ-23 ($\tau_1 = 13.3 \pm 1.3$ s and $\tau_2 = 792.6 \pm 131.7$ s), VPZ-34 ($\tau_1 = 19.4 \pm 1.4$ s and $\tau_2 = 692.6 \pm 77.9$ s), and VPZ-56 ($\tau_1 = 13.2 \pm 1.0$ s and $\tau_2 = 774.9 \pm 94.5$ s). (B) Time course of net CO₂ fixation rate in fully expanded leaves in response to a decrease in light intensity of 2000 to 200 $\mu\text{mol photons m}^{-2} \text{s}^{-1}$ at time zero, indicated by the black arrow. Error bars indicate SEM ($n = 5$ biological replicates). Asterisk indicates significant difference ($\alpha = 0.05$).

which can be induced by a number of different mechanisms with contrasting time constants (3). So-called energy-dependent quenching (qE) (10) requires low thylakoid lumen pH and is greatly aided by the presence of PSII subunit S (PsbS) (11, 12) and de-epoxidation of violaxanthin to antheraxanthin and zeaxanthin via the xanthophyll cycle (13, 14). Expression of PsbS strongly

affects the amplitude of qE formation, and overexpression results in an increased rate of induction and relaxation of qE (15–17). As a result, the effects of PsbS overexpression on CO₂ fixation and plant growth depend on the prevailing light environment. Enhancement of qE via PsbS overexpression may offer increased photoprotection under high light or rapidly fluctuating condi-

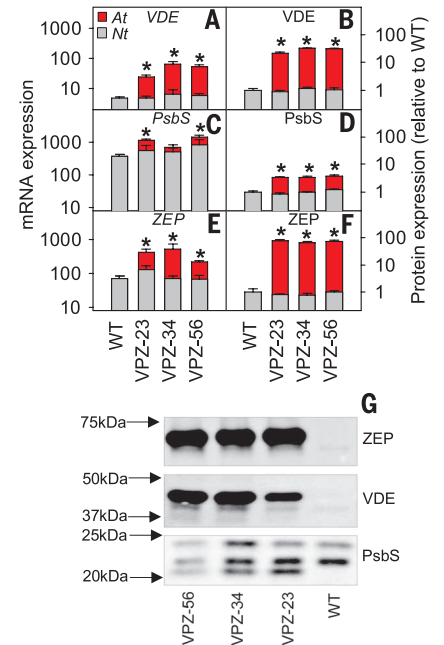


Fig. 2. Levels of mRNA and protein of VDE, PsbS, and ZEP. Native (Nt) and transgenic (At) VDE, PsbS, and ZEP in leaves of wild-type *N. tabacum* (WT) and three lines expressing *AtVDE*, *AtPsbS*, and *AtZEP* (VPZ) grown under greenhouse conditions. (A, C, and E) mRNA levels relative to actin and tubulin. (B, D, and F) Protein levels relative to WT, determined from densitometry on immunoblots. Error bars indicate SEM ($n = 5$ biological replicates), and asterisks indicate significant differences between VPZ lines and WT ($\alpha = 0.05$). (G) Representative immunoblots for VDE, PsbS, and ZEP.

tions (18) but can be at the expense of CO₂ fixation under less stressful conditions (15). An alternative route of NPQ manipulation is to modify xanthophyll cycle kinetics. The xanthophyll cycle de-epoxidation state (DES) influences the level of NPQ (19) because of the stimulating effect of zeaxanthin on qE and on zeaxanthin-dependent quenching (qZ) (20). qZ has slower relaxation kinetics (10 to 15 min) than qE (10 to 90 s), which are linked to the kinetics of the zeaxanthin pool. *Arabidopsis* mutants with increased xanthophyll-cycle pigment pool size were shown to have slower rates of NPQ formation and relaxation, owing to slower DES kinetics (21). Thus, the rate of adjustment of DES appears to be affected by the xanthophyll-cycle pool size relative to the rate of turnover via violaxanthin de-epoxidase (VDE) and zeaxanthin epoxidase (ZEP), which in turn affects the adjustment rate of NPQ.

We hypothesized that by accelerating the xanthophyll cycle and increasing PsbS, NPQ would decline more rapidly on transfer of leaves to shade (Fig. 1), leading to faster restoration of the maximum efficiency of CO₂ assimilation that can be achieved at a given light intensity in

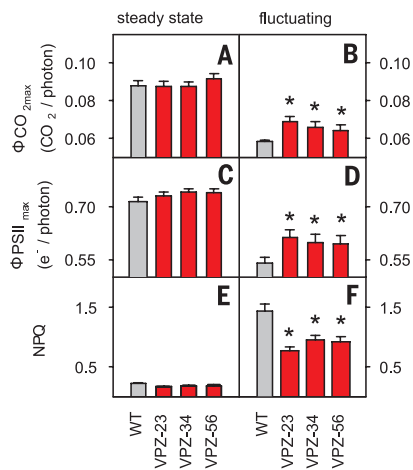


Fig. 4. Photosynthetic efficiency and NPQ under steady-state and fluctuating light. (A) Quantum efficiency of leaf net CO_2 assimilation ($\Phi\text{CO}_{2\text{max}}$) under steady-state light. (B) $\Phi\text{CO}_{2\text{max}}$ under fluctuating light. (C) Quantum efficiency of linear electron transport ($\Phi\text{PSII}_{\text{max}}$) under steady-state light. (D) Quantum efficiency of linear electron transport ($\Phi\text{PSII}_{\text{max}}$) under fluctuating light. (E) Average NPQ corresponding to (A) and (C). (F) Average NPQ corresponding to (B) and (D). Data were derived from light-response curves in which light intensity was either increased from low to high photon flux density (PFD), while waiting for steady state at each step (steady-state), or varied from high to low PFD with 4 min of $2000 \mu\text{mol photons m}^{-2} \text{s}^{-1}$ before each light-intensity change (fluctuating). Error bars indicate SEM ($n = 6$ biological replicates), and asterisks indicate significant differences ($\alpha = 0.05$) between wild-type *N. tabacum* (WT) and three lines expressing *AtVDE*, *AtPsbS*, and *AtZEP* (VPZ).

the shade, which in turn would allow increased productivity.

Results

Transgene mRNA and protein expression

Nicotiana tabacum was transformed with the coding sequences of *Arabidopsis VDE*, *ZEP*, and *PsbS* under the control of different promoters for expression in leaves (fig. S1). Two transformants with a single transfer DNA (T-DNA) integration (VPZ-34 and -56) and one transformant with two T-DNA insertions (VPZ-23) were selected based on a seedling NPQ screen (figs. S2 and S3) and self-pollinated to obtain homozygous T2 progeny for further investigation. All three VPZ lines showed increases in total (transgenic plus native) transcript levels of *VDE* (10-fold), *PsbS* (threefold), and *ZEP* (sixfold) relative to those of the wild type (WT) (Fig. 2, A, C, and E). For *PsbS*, the increase in transcript levels translated into an approximately fourfold-higher *PsbS* protein level (Fig. 2D), as exemplified in bands at 21 kDa (*AtPsbS*) and 24 kDa (*NtPsbS*) (Fig. 2G). For *VDE* and *ZEP*, the increase in transcript levels corresponded to 30-fold for *VDE* (45 kDa) (Fig. 2, B and G) and 74-fold for *ZEP* (73 kDa) (Fig. 2, F and G) increases over WT protein levels. Field-grown plants showed

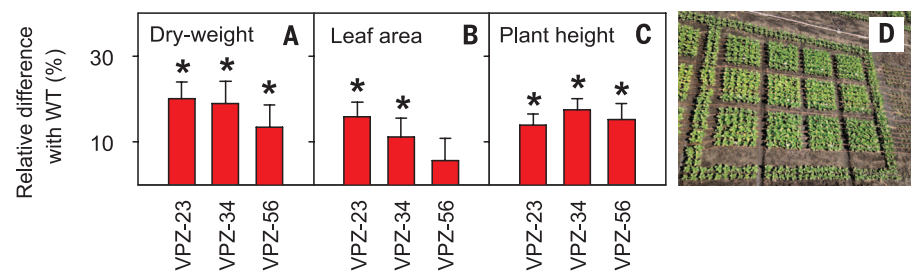


Fig. 5. Productivity of field-grown *N. tabacum* plants. Lines expressing *AtVDE*, *AtPsbS*, and *AtZEP* (VPZ) produced 15% larger plants than did the WT. (A) Total dry weight. (B) Leaf area. (C) Plant height. Data were normalized to WT. Error bars indicate SEM ($n = 12$ blocks), and asterisks indicate significant differences between VPZ lines and WT ($\alpha = 0.05$). (D) Aerial view of the field experiment in Urbana, Illinois (40.11°N , 88.21°W), in the summer of 2016. [Photo: D. Drag]

similar increases in protein levels (47-, 3-, and 75-fold for *VDE*, *PsbS*, and *ZEP*, respectively) (fig. S4), although increases in transcript levels were less pronounced (4-, 1.2-, and 7-fold for *VDE*, *PsbS*, and *ZEP*, respectively) (fig. S4).

Faster relaxation of NPQ and recovery of CO_2 fixation rate

To compare the kinetics of dynamic NPQ adjustment, a double exponential model was fitted to dark relaxation of NPQ in young seedlings after exposure to fluctuating light between 2000 and $200 \mu\text{mol photons m}^{-2} \text{s}^{-1}$ (Fig. 3A). The qZ phase of NPQ relaxation (τ_2) was significantly faster in VPZ lines at an average of 753 versus 2684 s in WT ($P < 0.05$), and qE relaxation (τ_1) was also noticeably faster at an average of 15 versus 21 s (significant in VPZ-23 and VPZ-56, $P < 0.05$). To see whether this faster relaxation translated into higher leaf CO_2 uptake, leaves were exposed to a sharp transition in light from 2000 to $200 \mu\text{mol photons m}^{-2} \text{s}^{-1}$. CO_2 assimilation declined immediately after the decrease in light intensity in both WT and VPZ lines (Fig. 3B), reaching a minimum at 30 s. During the following 150 s, the CO_2 fixation rate increased gradually but more rapidly in the VPZ lines as compared with WT, leading to significantly higher CO_2 fixation rates, averaging an increase of 9% ($P < 0.02$).

Effects of fluctuating light on the efficiency of photosynthetic CO_2 assimilation

To evaluate the dynamic effect of VPZ overexpression on the response of leaf CO_2 uptake to light, light intensity was varied in two different ways. First, light intensity was varied from low to high (fig. S5A), taking care to allow gas exchange and fluorescence to achieve steady state at each light intensity. Second, light intensity was varied in 4-min alternating steps of high to low light (fig. S5B). The resulting steady-state and fluctuating light-response curves of CO_2 fixation and linear electron transport rate were distinctly different between WT and VPZ lines. In steady state, the maximum quantum yield of CO_2 fixation ($\Phi\text{CO}_{2\text{max}}$) was not different between WT and VPZ lines, averaging $0.092 \text{ CO}_2/\text{absorbed photon}$ (Fig. 4A). Fluctuating light decreased $\Phi\text{CO}_{2\text{max}}$ to $0.058 \text{ CO}_2/$

absorbed photon in the WT plants (Fig. 4B), whereas $\Phi\text{CO}_{2\text{max}}$ in the VPZ lines showed a far smaller depression to $0.066 \text{ CO}_2/\text{absorbed photon}$ ($P < 0.05$). Similarly, under fluctuating light, the maximum quantum yield of whole-chain electron transport ($\Phi\text{PSII}_{\text{max}}$) declined from an average value of 0.73 (Fig. 4C) to $0.54 e^-/\text{absorbed photon}$ in the WT plants (Fig. 4D), compared with $0.60 e^-/\text{absorbed photon}$ in the VPZ lines ($P < 0.05$). Thus, under these fluctuating conditions, average $\Phi\text{CO}_{2\text{max}}$ and average $\Phi\text{PSII}_{\text{max}}$ of the VPZ lines were 11.3 and 14.0% higher than WT, respectively. These differences were also confirmed in plants grown under field conditions (fig. S6, A and B) and were not caused by a difference in photosynthetic capacity, as shown by the lack of differences in $\Phi\text{CO}_{2\text{max}}$ and $\Phi\text{PSII}_{\text{max}}$ between VPZ lines and WT when measured at steady state (Fig. 4, A and C). There were also no differences in the maximum carboxylation capacity (V_{cmax}) or ribulose biphosphate regeneration capacity (J_{max}) derived from CO_2 response curves (table S1), nor were there differences in the levels and stoichiometry of the major photosynthetic complexes (fig. S7). Instead, the differences under fluctuating conditions corresponded to the faster relaxation of NPQ resulting from VPZ overexpression. Steady-state NPQ below $400 \mu\text{mol photons m}^{-2} \text{s}^{-1}$ was very low (Fig. 4E and fig. S5G) and did not differ between WT and VPZ lines. However, under fluctuating light intensity, NPQ was significantly higher in the WT compared with the VPZ lines at low light ($P < 0.05$) (Fig. 4F), whereas NPQ in high light did not differ between WT and VPZ lines (fig. S5, G and H).

Productivity under field conditions

Whether this greater photosynthetic efficiency during shading events would affect productivity was evaluated under field conditions in a randomized block design with 12 blocks (Fig. 5D and fig. S8). Plants from VPZ lines exhibited greater total dry weight per plant by 14 to 20% relative to that of WT (Fig. 5A), which was evident in increases in leaf, stem, and root weights (fig. S9, A to C). Additionally, plants from VPZ lines showed increases in leaf area (Fig. 5B) and plant height (Fig. 5C), relative to WT. Similar productivity increases were found under greenhouse conditions (fig. S10, A to F).

Table 1. Xanthophyll cycle pigment concentrations and DES. Samples were taken from greenhouse-grown fully expanded leaves of wild-type *N. tabacum* (WT) and three lines overexpressing *AtVDE*, *AtPsbS*, and *AtZEP* (VPZ) in dark-acclimated state or after exposure to constant 400 or 2000 $\mu\text{mol photons m}^{-2} \text{s}^{-1}$ (when steady-state photosynthesis was reached) or three cycles of 3 min 2000/3 min 200 $\mu\text{mol photons m}^{-2} \text{s}^{-1}$. Pigment concentrations (mean \pm SEM, $n = 3$ to 6 biological replicates) were normalized by chlorophyll a content (mmol mol^{-1}). Asterisks indicate significant differences between VPZ lines and WT ($\alpha = 0.05$). Vio, violaxanthin; Ant, antheraxanthin; Zea, zeaxanthin; DES (%), $(\text{Zea} + 0.5\text{Ant})/(\text{Zea} + \text{Ant} + \text{Vio})$; n.d., not detected.

Light treatment	Pigment	WT	VPZ-23	VPZ-34	VPZ-56
Dark-acclimated	Vio	68.6 \pm 1.5	52.1 \pm 1.7	48.5 \pm 0.6	51.6 \pm 1.7
	Ant	0.1 \pm 0.0	0.0 \pm 0.0	0.0 \pm 0.0	0.0 \pm 0.0
	Zea	n.d.	n.d.	n.d.	n.d.
	DES	0	0	0	0
Constant at 400 $\mu\text{mol photons m}^{-2} \text{s}^{-1}$	Vio	53.0 \pm 1.7	54.1 \pm 6.2	56.9 \pm 1.1	53.2 \pm 1.2
	Ant	0.2 \pm 0.1	0.1 \pm 0.0	0.1 \pm 0.0	0.1 \pm 0.0
	Zea	1.7 \pm 0.8	0.0 \pm 0.0	0.4 \pm 0.4	0.0 \pm 0.0
	DES	3.0 \pm 1.5	0.0 \pm 0.0	0.7 \pm 0.7	0.1 \pm 0.0
Constant at 2000 $\mu\text{mol photons m}^{-2} \text{s}^{-1}$	Vio	29.0 \pm 1.3	36.7 \pm 4.5	30.1 \pm 1.4	34.3 \pm 0.4
	Ant	0.5 \pm 0.0	0.6 \pm 0.1	0.5 \pm 0.0	0.6 \pm 0.1
	Zea	26.3 \pm 1.8	*11.1 \pm 3.6	*11.3 \pm 2.6	*14.1 \pm 3.8
	DES	46.3 \pm 2.7	*22.7 \pm 7.5	*26.0 \pm 5.3	*27.7 \pm 5.2
Fluctuating between 2000 and 200 $\mu\text{mol photons m}^{-2} \text{s}^{-1}$	Vio	21.0 \pm 0.6	*35.8 \pm 1.2	*28.7 \pm 1.6	*31.9 \pm 0.9
	Ant	0.8 \pm 0.1	*0.5 \pm 0.0	0.7 \pm 0.1	*0.4 \pm 0.1
	Zea	24.9 \pm 2.1	*4.7 \pm 0.3	*11.4 \pm 3.8	*6.6 \pm 1.0
	DES	52.4 \pm 2.4	*11.3 \pm 0.5	*25.5 \pm 7.0	*16.4 \pm 1.9

Xanthophyll cycle de-epoxidation as a function of different light treatments

In dark-acclimated leaves from both WT and VPZ lines, the xanthophyll-cycle pool was completely epoxidated—entirely in the form of violaxanthin (Table 1). Exposure to 400 $\mu\text{mol photons m}^{-2} \text{s}^{-1}$ constant light did not lead to substantial de-epoxidation, but 2000 $\mu\text{mol photons m}^{-2} \text{s}^{-1}$ constant light led to accumulation of antheraxanthin and especially zeaxanthin. VPZ lines retained more violaxanthin and accumulated less zeaxanthin and antheraxanthin compared with that of WT, which led DES in the VPZ lines to be about half that of WT (26 versus 46%). Exposure to fluctuating light led to similar results as high light exposure, but with even less xanthophyll de-epoxidation in the VPZ lines, relative to WT (18 versus 53%), and field-grown plants of VPZ-23 showed significantly lower DES than that of WT throughout a diurnal period ($P < 0.05$) (fig. S11). Because of the lower DES in the VPZ lines, a concern was that they would be more vulnerable to photo-inhibition. However, photoprotection in seedlings after 2 hours exposure to excessive light ($\lambda_{\text{max}} = 470 \text{ nm}$, 2000 $\mu\text{mol photons m}^{-2} \text{s}^{-1}$) appeared to be equal (VPZ-56) or even higher (VPZ-23 and VPZ-34; $P < 0.05$) than that in WT (fig. S12).

Discussion

How does introduction of the VPZ construct accelerate NPQ relaxation on transfer of leaves from high to low light, as would occur in a shading event? NPQ is a compound variable,

encompassing several quenching mechanisms with contrasting relaxation kinetics (22). Whereas PsbS is exclusively associated with rapidly relaxing qE, the xanthophyll cycle is involved in multiple components of NPQ, especially qE and qZ. Even though VPZ lines had a lower xanthophyll DES under high and fluctuating light intensity (Table 1), levels of NPQ were similar to those of WT at high light (figs. S3B and S5H), implying that the relationship between xanthophyll DES and NPQ has been altered by PsbS overexpression, allowing for higher NPQ at lower DES. The presence of zeaxanthin correlates with faster induction and slower relaxation of NPQ, with respect to qZ and qE (4, 20, 23). Consistent with the lower DES in the VPZ lines, relaxation of both qE (τ_1) and qZ (τ_2) was accelerated by the VPZ overexpression. The faster relaxation of NPQ by VPZ overexpression can thus be explained by two parallel manipulations of NPQ. Combined overexpression of VDE and ZEP decreased xanthophyll DES, which in turn increased the NPQ relaxation rate through qZ, qE, and zeaxanthin-associated effects on NPQ kinetics. Second, the overexpression of PsbS led to an increase in qE, which more than offset the decrease due to lower DES (fig. S3B).

The hypothesis that photosynthetic efficiency could be increased through acceleration of NPQ relaxation (8, 24) relies on the inverse correlation between NPQ and photosynthetic efficiency. Under fluctuating light, the VPZ lines showed faster and greater decreases in NPQ after transitions from high to low light, relative to that of WT (Fig. 4F and fig. S5H), which increased

the quantum yield of CO_2 assimilation by 14% (Fig. 4B), providing proof that on transition from high to low light, NPQ does indeed limit photosynthetic efficiency. Xanthophyll DES is correlated with NPQ (19), which suggests that limiting violaxanthin de-epoxidation may also increase the NPQ relaxation rate. However, decreased zeaxanthin formation through antisense *VDE* expression in tobacco in previous studies did not lead to an increase in photosynthetic efficiency and growth (25, 26). Reduction in NPQ amplitude (27) and antioxidant capacity (28) leads to greater sensitivity to damage by excessive light in mutants with reduced zeaxanthin (29). In the current work, expression of VDE and PsbS was increased to balance the up-regulation of ZEP and avoid such damage (fig. S12). This conservation of photoprotection in the VPZ lines most likely originates from an increase in qE, reflecting the positive correlation between photoprotection and PsbS content (18).

About 50% of canopy carbon gain in crops occurs under light limitation (5). Efficiency of photosynthesis in the shade declines even further with rapid light transitions caused by clouds and wind-driven movement of overshadowing leaves. Higher yields have followed increased planting densities, which also caused denser canopies and increased the proportion of partially shaded leaves, leading to more irregular light conditions for each leaf. Even on a clear day, diurnal changes in sun angle cause dynamic shading of leaves within the canopy by those at the top. At the level of the individual chloroplast, these changes from sun to shade are almost instantaneous (7). Thus, light conditions in the field are anything but steady state. Under steady-state light, the VPZ lines evaluated here would have shown no yield advantage over WT. Their yield advantage becomes apparent under more realistic, irregular, lighting conditions.

Because the xanthophyll cycle and PsbS are common to all vascular plants (11, 19), we expect that similar results would pertain to all major crops. Although this work has focused on crop light-use efficiency, stomatal conductance also remains high during the first few minutes after transfer to shade. Increasing the rate of relaxation of NPQ will therefore not only increase net carbon gain but also increase crop water-use efficiency. This may be an important attribute, given forecast climate change impacts on future crop production (30).

Transgenic expression of *Arabidopsis* VDE, PsbS, and ZEP (VPZ) in combination in tobacco led to a marked and statistically significant acceleration of NPQ relaxation on transfer of leaves from high light to shade. As hypothesized, this led to a more rapid recovery of the efficiency of photosynthetic CO_2 assimilation in the shade. Results from field and greenhouse experiments showed that this corresponded to increased productivity in terms of final dry mass. Increases in crop productivity of 15%, as obtained here, demonstrate a potential means to achieve the increases in crop yield that are forecast to be necessary by 2050 (31, 32).

REFERENCES AND NOTES

1. D. R. Ort et al., *Proc. Natl. Acad. Sci. U.S.A.* **112**, 8529–8536 (2015).
2. Z. Li, S. Wakao, B. B. Fischer, K. K. Niyogi, *Annu. Rev. Plant Biol.* **60**, 239–260 (2009).
3. P. Müller, X.-P. Li, K. K. Niyogi, *Plant Physiol.* **125**, 1558–1566 (2001).
4. M. L. Pérez-Bueno, M. P. Johnson, A. Zia, A. V. Ruban, P. Horton, *FEBS Lett.* **582**, 1477–1482 (2008).
5. S. P. Long, S. Humphries, P. G. Falkowski, *Annu. Rev. Plant Biol.* **45**, 633–662 (1994).
6. C. Werner, R. J. Ryel, O. Correia, W. Beyschlag, *Plant Cell Environ.* **24**, 27–40 (2001).
7. X.-G. Zhu, D. R. Ort, J. Whitmarsh, S. P. Long, *J. Exp. Bot.* **55**, 1167–1175 (2004).
8. E. H. Murchie, K. K. Niyogi, *Plant Physiol.* **155**, 86–92 (2011).
9. C. D. P. Duffy, A. V. Ruban, *J. Photochem. Photobiol. B* **152** (pt. B), 215–226 (2015).
10. C. A. Wraight, A. R. Crofts, *Eur. J. Biochem.* **17**, 319–327 (1970).
11. M. D. Brooks, S. Jansson, K. K. Niyogi, in *Non-Photochemical Quenching and Energy Dissipation in Plants Algae and Cyanobacteria* (Springer, 2014), vol. 40, pp. 297–314.
12. X.-P. Li et al., *Nature* **403**, 391–395 (2000).
13. B. Demmig-Adams, *Biochim. Biophys. Acta* **1020**, 1–24 (1990).
14. H. Y. Yamamoto, T. O. M. Nakayama, C. O. Chichester, *Arch. Biochem. Biophys.* **97**, 168–173 (1962).
15. S. Hubbard, O. O. Ajigboye, P. Horton, E. H. Murchie, *Plant J.* **71**, 402–412 (2012).
16. X.-P. Li, A. M. Gilmore, K. K. Niyogi, *J. Biol. Chem.* **277**, 33590–33597 (2002).
17. A. Zia, M. P. Johnson, A. V. Ruban, *Planta* **233**, 1253–1264 (2011).
18. X.-P. Li, P. Muller-Moule, A. M. Gilmore, K. K. Niyogi, *Proc. Natl. Acad. Sci. U.S.A.* **99**, 15222–15227 (2002).
19. B. Demmig-Adams, W. W. Adams III, *Planta* **198**, 460–470 (1996).
20. M. Nilkens et al., *Biochim. Biophys. Acta* **1797**, 466–475 (2010).
21. M. P. Johnson, P. A. Davison, A. V. Ruban, P. Horton, *FEBS Lett.* **582**, 262–266 (2008).
22. A. V. Ruban, *Plant Physiol.* **170**, 1903–1916 (2016).
23. P. Horton, A. V. Ruban, R. G. Walters, *Annu. Rev. Plant Physiol. Plant Mol. Biol.* **47**, 655–684 (1996).
24. S. P. Long, X.-G. Zhu, S. L. Naidu, D. R. Ort, *Plant Cell Environ.* **29**, 315–330 (2006).
25. S.-H. Chang, R. C. Bugos, W.-H. Sun, H. Y. Yamamoto, *Photosynth. Res.* **64**, 95–103 (2000).
26. W.-H. Sun, A. S. Verhoeven, R. C. Bugos, H. Y. Yamamoto, *Photosynth. Res.* **67**, 41–50 (2001).
27. K. K. Niyogi, A. R. Grossman, O. Björkman, *Plant Cell* **10**, 1121–1134 (1998).
28. M. Havaux, L. Dall'osto, R. Bassi, *Plant Physiol.* **145**, 1506–1520 (2007).
29. N. Wang et al., *Physiol. Plant.* **132**, 384–396 (2008).
30. D. R. Ort, S. P. Long, *Science* **344**, 484–485 (2014).
31. J. Kromdijk, S. P. Long, *Proc. Biol. Sci.* **283**, 20152578 (2016).
32. D. Tilman, M. Clark, *Daedalus* **144**, 8–23 (2015).

ACKNOWLEDGMENTS

We thank D. Drag and B. Harbaugh for plant management in greenhouse and field studies; M. Kobayashi for performing the high-performance liquid chromatography analysis of pigments from the field-grown plants; and K. Kucera, M. Steiner, and S. Gillespie for general assistance during laboratory- and fieldwork. We also thank T. Clemente for initial help with tobacco transformation. This research was supported by Bill and Melinda Gates Foundation grant OPP1060461, titled “RIPE—Realizing increased photosynthetic efficiency for sustainable increases in crop yield.” K.K.N. is an investigator of the Howard Hughes Medical Institute and the Gordon and Betty Moore Foundation (through grant GBMF3070). The data reported in this paper have been tabulated in the supplementary materials. Plants and constructs reported are available from the University of Illinois and University of California, Berkeley, for research purposes, subject to the conditions of the Uniform Biological Material Transfer Agreement. The University of Illinois has submitted a provisional patent on behalf of J.K., K.G., L.L., K.K.N., and S.P.L. on aspects of the findings.

SUPPLEMENTARY MATERIALS

www.sciencemag.org/content/354/6314/857/suppl/DC1

Materials and Methods

Figs. S1 to S14

Tables S1 to S3

Data Sets 1 to 21

References (33–49)

29 August 2016; accepted 28 September 2016

10.1126/science.aai8878

REPORTS

SOLAR CELLS

Perovskite-perovskite tandem photovoltaics with optimized band gaps

Giles E. Eperon,^{1,2*} Tomas Leijtens,^{3*} Kevin A. Bush,³ Rohit Prasanna,³ Thomas Green,¹ Jacob Tse-Wei Wang,¹ David P. McMeekin,¹ George Volonakis,⁴ Rebecca L. Milot,¹ Richard May,² Axel Palmstrom,⁵ Daniel J. Slotcavage,³ Rebecca A. Belisle,³ Jay B. Patel,¹ Elizabeth S. Parrott,¹ Rebecca J. Sutton,¹ Wen Ma,⁶ Farhad Moghadam,⁶ Bert Conings,^{1,7} Aslihan Babayigit,^{1,7} Hans-Gerd Boyen,⁷ Stacey Bent,⁵ Feliciano Giustino,⁴ Laura M. Herz,¹ Michael B. Johnston,¹ Michael D. McGehee,^{2†} Henry J. Snaith^{1†}

We demonstrate four- and two-terminal perovskite-perovskite tandem solar cells with ideally matched band gaps. We develop an infrared-absorbing 1.2-electron volt band-gap perovskite, $\text{FA}_{0.75}\text{Cs}_{0.25}\text{Sn}_{0.5}\text{Pb}_{0.5}\text{I}_3$, that can deliver 14.8% efficiency. By combining this material with a wider-band gap $\text{FA}_{0.83}\text{Cs}_{0.17}\text{Pb}(\text{I}_{0.5}\text{Br}_{0.5})_3$ material, we achieve monolithic two-terminal tandem efficiencies of 17.0% with >1.65-volt open-circuit voltage. We also make mechanically stacked four-terminal tandem cells and obtain 20.3% efficiency. Notably, we find that our infrared-absorbing perovskite cells exhibit excellent thermal and atmospheric stability, not previously achieved for Sn-based perovskites. This device architecture and materials set will enable “all-perovskite” thin-film solar cells to reach the highest efficiencies in the long term at the lowest costs.

Metal halide perovskites [ABX_3 , where A is typically Cs, methylammonium (MA), or formamidinium (FA); B is Pb or Sn; and X is I, Br, or Cl] have emerged as an extremely promising photovoltaic (PV) technology owing to their rapidly increasing power conversion efficiencies (PCEs) and low processing costs. Single-junction perovskite devices have reached a certified 22% PCE (1), but the first commercial iterations of perovskite PVs will likely be as an “add-on” to silicon (Si) PVs. In a tandem configuration, a perovskite with a band gap of ~1.75 eV can enhance the efficiency of the silicon cell. (2) An all-perovskite tandem cell could deliver lower fabrication costs, but requires band gaps that have not yet been realized. The highest-efficiency tandem devices would require a rear cell with a band gap of 0.9 to 1.2 eV and a front cell with a band gap of 1.7 to 1.9 eV. Although materials such

as $\text{FA}_{0.83}\text{Cs}_{0.17}\text{Pb}(\text{I}_x\text{Br}_{1-x})_3$ deliver appropriate band gaps for the front cell (2), Pb-based materials cannot be tuned to below 1.48 eV for the rear cell. Completely replacing Pb with Sn can shift the band gap to ~1.3 eV (for MASnI_3) (3), but the tin-based materials are notoriously air sensitive and difficult to process, and PV devices based on them have been limited to ~6% PCE. (3, 4) An anomalous band-gap bowing in mixed tin-lead perovskite systems ($\text{MAPb}_{0.5}\text{Sn}_{0.5}\text{I}_3$) has given band gaps of ~1.2 eV but mediocre performance (~7% PCE). Very recently, PCE of >14% has been reported with $\text{MA}_{0.5}\text{FA}_{0.5}\text{Pb}_{0.75}\text{Sn}_{0.25}\text{I}_3$ cells, for band gaps >1.3 eV and all-perovskite four-terminal tandem cells with 19% efficiency (5, 6, 7). Here, we demonstrate a stable, 14.8% efficient perovskite solar cell based on a ~1.2-eV band gap $\text{FA}_{0.75}\text{Cs}_{0.25}\text{Pb}_{0.5}\text{Sn}_{0.5}\text{I}_3$ absorber. We measure open-circuit voltages (V_{oc} 's) of up to 0.83 V in these cells, which represents a smaller voltage deficit between band gap and V_{oc} than measured for the highest-efficiency lead-based perovskite cells. We then combined these with 1.8-eV $\text{FA}_{0.83}\text{Cs}_{0.17}\text{Pb}(\text{I}_{0.5}\text{Br}_{0.5})_3$ perovskite cells, to demonstrate current-matched and efficient (17.0% PCE) monolithic all-perovskite two-terminal tandem solar cells on small areas and 13.8% PCE on large areas, with V_{oc} >1.65 V. Finally, we fabricated 20.3% efficient small-area and 16.0% efficient 1-cm² all-perovskite four-terminal tandems using a semitransparent 1.6-eV $\text{FA}_{0.83}\text{Cs}_{0.17}\text{Pb}(\text{I}_{0.83}\text{Br}_{0.17})_3$ front cell.

¹Department of Physics, University of Oxford, Clarendon Laboratory, Parks Road, Oxford OX1 3PU, UK. ²Department of Chemistry, University of Washington, Seattle, WA, USA.

³Department of Materials Science, Stanford University, Lomita Mall, Stanford, CA, USA. ⁴Department of Materials, University of Oxford, Parks Road, Oxford OX1 3PH, UK.

⁵Department of Chemical Engineering, Stanford University, Via Ortega, Stanford, CA, USA. ⁶SunPreme, Palomar Avenue, Sunnyvale, CA, USA. ⁷Institute for Materials Research, Hasselt University, Diepenbeek, Belgium.

*These authors contributed equally to this work. †Corresponding author. Email: mmcgehee@stanford.edu (M.D.M.); henry.snaith@physics.ox.ac.uk (H.J.S.)

EXTENDED PDF FORMAT
SPONSORED BY



Improving photosynthesis and crop productivity by accelerating recovery from photoprotection

Johannes Kromdijk, Katarzyna Glowacka, Lauriebeth Leonelli, Stéphane T. Gabilly, Masakazu Iwai, Krishna K. Niyogi and Stephen P. Long (November 17, 2016)
Science **354** (6314), 857-861. [doi: 10.1126/science.aai8878]

Editor's Summary

Faster light adaptation improves productivity

Crop plants protect themselves from excess sunlight by dissipating some light energy as heat, readjusting their systems when shadier conditions prevail. But the photosynthetic systems do not adapt to fluctuating light conditions as rapidly as a cloud passes overhead, resulting in suboptimal photosynthetic efficiency. Kromdijk *et al.* sped up the adaptation process by accelerating interconversion of violaxanthin and zeaxanthin in the xanthophyll cycle and by increasing amounts of a photosystem II subunit. Tobacco plants tested with this system showed about 15% greater plant biomass production in natural field conditions.

Science, this issue p. 857

This copy is for your personal, non-commercial use only.

Article Tools Visit the online version of this article to access the personalization and article tools:
<http://science.sciencemag.org/content/354/6314/857>

Permissions Obtain information about reproducing this article:
<http://www.sciencemag.org/about/permissions.dtl>

Science (print ISSN 0036-8075; online ISSN 1095-9203) is published weekly, except the last week in December, by the American Association for the Advancement of Science, 1200 New York Avenue NW, Washington, DC 20005. Copyright 2016 by the American Association for the Advancement of Science; all rights reserved. The title *Science* is a registered trademark of AAAS.